Green Chemistry

Accepted Manuscript

This article can be cited before page numbers have been issued, to do this please use: M. Lu, J. Zhang, Y. Yao, J. Sun, Y. Wang and H. Lin, *Green Chem.*, 2018, DOI: 10.1039/C8GC00954F.

ROYAL SOCIETY OF CHEMISTRY

rsc.li/green-chem

View Article Online
DOI: 10.1039/C8GC00954F

Green Chemistry

COMMUNICATION

Renewable Energy Storage via Efficient Reversible Hydrogenation of Piperidine Captured CO_2

Received 00th January 20xx,
Accepted 00th January 20xx

DOI: 10.1039/x0xx00000x

www.rsc.org/

Mi Lu, Jianghao Zhang, Yao Yao, Junming Sun, Yong Wang, and Hongfei Lin*

The storage of renewable energy is the major hurdle during the transition of fossil resources to renewables. A possible solution is to convert renewable electricity to chemical energy carriers such as hydrogen for storage. Herein, a highly efficient formate-piperidine-adduct (FPA) based hydrogen storage system was developed. This system has shown rapid reaction kinetics of both the hydrogenation of piperidine captured CO_2 and the dehydrogenation of FPA over the carbon-supported palladium nano-catalyst under mild operating conditions. Moreover, the FPA solution based hydrogen storage system is advantageous owing to the generation of high-purity hydrogen, which is free of carbon monoxide and ammonia. The in-situ ATR-FTIR characterization was performed in order to provide insight into the reaction mechanisms involved. By integrating this breakthrough hydrogen storage system with renewable hydrogen, and the polymer electrolyte membrane fuel cells (PEMFC), the on demand cost-effective rechargeable hydrogen battery could be realized for renewable energy storage.

The worldwide installed solar photovoltaic (PV) and wind energy capacity have surged exponentially for the past decades.[1] However, the wind and solar power generation are highly intermittent and seasonal, resulting in serious issues including grid capacity/stability, curtailment, and supply/demand mismatch. One possible solution to the renewable electricity storage challenge is to use a regenerative hydrogen fuel cell (RHFC), which converts electricity to H_2, a clean energy carrier that can be obtained from electrochemical water splitting,[2] and stores the H_2, which is later fed into a fuel cell to regenerate electric power.[3] Currently, hydrogen gas is commonly compressed and stored at extremely high pressure (700 bar), leading to a high cost, as well as safety concerns and logistical challenges since it is highly inflammable.[4] Chemical hydrogen storage options, including solid-state metal hydrides or liquid organic hydrogen carriers (LOHCs), could be a safe alternative to hydrogen storage,[4c, 5]. However, the hydrogen release from these materials is strongly endothermic, typically requiring elevated temperatures of 150~500 ºC, which are well above the "waste heat" temperature range of 80~90 ºC provided by a standard PEMFC.

Formic acid (HCOOH) and formates have been considered as a promising material for chemical hydrogen storage because their high volumetric capacities, which surpass those of most other chemical hydrogen storage materials.[6] Recently, immense progress has been made on the development of formate-based reversible H_2 storage at mild conditions.[2b, 7] Beller and co-workers suggested that the catalytic decomposition of a formate/amine adduct solution in the presence of the homogeneous Ru catalysts as a practical H_2 storage system for direct use in fuel cells.[8] Hull *et al.* designed a reversible H_2 storage system with a homogenous Ir catalyst, using pH to control H_2 production or consumption.[9] Several reports also described the feasibility of using a homogeneous Ru catalyst to enable a reversible HCOONa/$NaHCO_3$-based H_2 storage to achieve a higher volumetric density.[10] Laurenczy's group designed a hydrogen battery system based on cesium formate/bicarbonate due to the high solubility of cesium salts.[7c] However, due to the high cost arising from the use of sophisticated ligands and the limited recyclability, the homogeneous catalyst systems have not yet been ready for commercial applications.

Compared to the significant advances of homogeneously catalyzed formate-based hydrogen storage systems, only few reports of using heterogeneous catalysts for hydrogen storage are available in the literature. Cao and co-workers[11] employed aqueous sodium formates as the H_2 storage material over the palladium on reduced graphitic oxide nanosheets (Pd/r-GO).[1c] Notably, the rate of hydrogen discharge is too low for practical application.[12] Recently, our group demonstrated a hydrogen storage system based on ammonium bicarbonate/formate redox equilibrium[7d] in aqueous media over the heterogeneous

The Gene and Linda Voiland School of Chemical Engineering and Bioengineering
Washington State University
Pullman WA 99164, USA
**Correspondence: Hongfei.Lin@wsu.edu*
† Footnotes relating to the title and/or authors should appear here.
Electronic Supplementary Information (ESI) available: [details of any supplementary information available should be included here]. See DOI: 10.1039/x0xx00000x

View Article Online
DOI: 10.1039/C8GC00954F

Pd/AC catalyst. This hydrogen storage system has an exceptionally high volumetric energy density (up to 168 g H_2/L). However, the challenge that the trace amounts of CO and NH_3 could be formed by decomposition of ammonium formate at elevated temperatures cannot be completely ruled out.[4c, 9f, 13] To further increase the power density, we found that adding alcohol as a co-solvent greatly enhances the kinetics of hydrogenation of ammonium carbonate.[14] Herein, we have developed a new hydrogen storage system based on the formate piperidine adduct (FPA) solutions, in which the fast hydrogenation of captured CO_2 with piperidine to FPA, as well as the rapid decomposition of FPA for releasing high-purity H_2, could be realized under mild conditions.

Table 1 shows the results of catalytic hydrogenation of piperidine captured CO_2 in various aqueous ethanol solutions. After reacting for 1 hour in water at 20 °C (Table 1, entry 1), the yield of formate was 50.2%, and the corresponding turnover frequency (TOF) was approximately 1431 h^{-1} over the activated carbon supported palladium catalyst (5 wt% Pd/AC). Adding alcohol into water solvent significantly improved the hydrogenation of piperidine captured CO_2. For instance, the ethanol-water solution with 70 wt% ethanol exhibited the significant solvent promotion effect as a high yield to formate of ~83.6% was achieved in an hour at 20 °C, and the TOF reached up to ~3523 h^{-1} over the Pd/AC catalyst (Table 1, entry 3). Moreover, a much higher yield of ~95.5% of formate was achieved by simply elevating the temperature from 20 °C to 30 °C (Table 1, entry 5). We found that other alcohols also have the similar promotion effect as ethanol. At 30 °C, by switching the aqueous ethanol solvent to the aqueous 1-propanol or the aqueous 2-propanol solvents, each containing 70 wt% alcohol, the formate yields reached ~96.4% and ~98.5%, respectively, in an hour (Table 1, entries 7 and 8).

higher solubility of H_2 in ethanol than in water;[15] and 2) the amount of bicarbonate and ethyl carbonate intermediate species which can be hydrogenated. Indeed, we observed an increasing trend of the formate yield as the ethanol content in the aqueous solutions increased from 0% to 70%, but the yield then decreased as the ethanol content further increased to 100%. The ^{13}C NMR characterization (Supporting Information Figure S1) found that there was only one peak located at 161.2 ppm which was assigned to the bicarbonate/carbonate ions after capturing CO_2 with piperidine in pure water.[16] In the ethanol-water mixed solvent, another peak located at 159.5 ppm appeared, which was referred to ethyl carbonate ions. In pure ethanol, only the ethyl carbonate peak displayed. This observation is well consistent with our previous report that ethyl carbonate ions present in the NH_4HCO_3 aqueous solutions when adding ethanol.[14] However, the yield of formate decreased from ~83.6% in the aqueous ethanol solvent (an ethanol fraction of 70 wt%) to ~62.2% in pure ethanol, implying that an appropriate amount of water may enhance the hydrogenation performance. Interestingly, the similar promotion effects by adding small amounts of water were observed in the CO_2 hydrogenation reactions with the homogeneous catalysts.[17] In general, under the identical conditions, the maximum formate yield was obtained with the aqueous ethanol solvent at an optimal ethanol to water ratio, rather than with pure ethanol. However, the different properties of the solvents at various ethanol to water ratios likely influence the solubility of hydrogen, as well as the distribution of the bicarbonate and ethyl carbonate ions in the ethanol-water solvents, and therefore determine the optimal yield of formate.

Table 1. Hydrogenation of piperidine captured CO_2 in different aqueous alcohol solutions.

Entry	Capture [a] and Hydrogenation[b] Solvent (wt% alcohol)	Temperature (°C)	Captured CO_2 species concentration (M)[c] HCO_3^-	CO_3^{2-}	$RNCO^{2-}$	*Alkyl*-CO_3^-	Conversion results Formate Yield (%)	TOF (h^{-1})[d]
1	0% alcohol	20	0.93	0.03	0.00	0	50.2	1431
2	50% EtOH	20	0.73	0.01	0.01	0.21	78.0	3303
3	70% EtOH	20	0.32	0.00	0.03	0.61	83.6	3523
4	70% EtOH	25	0.32	0.00	0.03	0.61	87.4	4404
5	70% EtOH	30	0.32	0.00	0.03	0.61	95.5	5945
6	70% EtOH	40	0.32	0.00	0.03	0.61	70.5	3083
7	70% 1-Propanol	30	0.30	0.00	0.03	0.62	96.4	4404
8	70% 2-Propanol	30	0.30	0.00	0.03	0.62	98.5	5504
9	90% EtOH	20	0.03	0.00	0.03	0.90	80.4	3083
10	95.6% EtOH	20	0.01	0.00	0.03	0.92	68.6	2642
11	100% EtOH	20	0.00	0.00	0.03	0.93	62.2	2202

[a] CO_2 capture conditions: 20 mL amine/water-ethanol, 1 M piperidine, 20 °C, 40 min.

[b] Hydrogenation conditions: 50 mL Parr reactor, captured CO_2 solution (20 mL), 0.1 g Pd/AC(5 wt%), 400 psi hydrogen, 1 hour, 20°C except entries 4-6.

[c] The captured CO_2 species concentrations were determined by ^{13}C NMR spectroscopy.

[d] The TOFs was calculated by: Moles of formate/(Moles of Pd × 23.2 %)/Reaction time. The dispersion of Pd atoms on the surface of Pd NPs is 23.2% which is determined by carbon monoxide chemisorption.

In our previous studies, we considered that the promotion effect of the ethanol co-solvent can be attributed to: 1) the

View Article Online
DOI: 10.1039/C8GC00954F

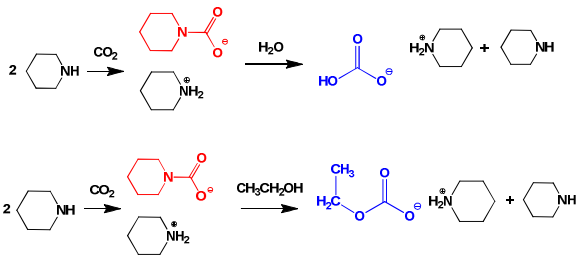

Scheme 1. Proposed mechanism of the formation of piperidine-carbamate by capturing CO_2 with piperidine and the subsequent conversion of piperidine-carbamate to the corresponding bicarbonate and ethyl carbonate salts in water and ethanol solvents, respectively.

Note that piperidine-carbamate was not observed from the *ex-situ* ^{13}C NMR characterization, although carbamate is readily formed by reacting CO_2 with piperidine, a highly basic amine[18] (p*Ka* = 11.28). Given the extended time (capturing CO_2 with piperidine lasted for 40 mins in this study), the piperidine-carbamate could be fully converted to bicarbonate[19] or ethyl carbonate in water or ethanol, respectively (Scheme 1). We also found that the CO_2 hydrogenation rates were faster with piperidine than those with AMP under the identical reaction conditions. Due to its strong basicity, piperidine acts as an electron-donating ligand which reduces the bonding energy of the formates on Pd surface and thus could improve the hydrogenation activity by enhancing the formate desorption, if the formate desorption would be the rate-limiting step. At the same time, the electron donating piperidine also decreases the electron deficient character of the Pd nanocatalysts.[20] Therefore, it is also possible that piperidine altered the electronic states of the Pd and thus promoted the hydrogenation reactions.

The temperature effect of hydrogenation of piperidine captured CO_2 was shown in Table 1 (Entries 3-6). The formate yield increased with increasing the reaction temperature from 20 °C to 30 °C, but then decreased with further increasing the reaction temperature to 40 °C. Generally speaking, higher reaction temperatures lead to faster hydrogenation kinetics. However, from the thermodynamics point of view, elevated temperatures favor the dehydrogenation reaction and thus shift the equilibrium to hydrogen evolution, which is in agreement with our previous study and the reports in the literature.[21] The detailed kinetic study on the hydrogenation of bicarbonate in pure water and ethyl carbonate in pure ethanol respectively, has been performed. Both bicarbonate and ethyl carbonate were derived from piperidine captured CO_2. As shown in Figure 1, in the temperature range of 20–40 °C, the activation energy (E_a) is 64.1±2.1 kJ/mol for the conversion of bicarbonate to formate in water, while it is slightly lower, 56.2±3.2 kJ/mol, for the hydrogenation of ethyl carbonate in absolute ethanol. Unlike the comparable activation energies of both reactions, the observed rate of the hydrogenation of ethyl carbonate in ethanol was an order of magnitude larger than that of the hydrogenation of bicarbonate in water, which likely due to the increased solubility of H_2 in ethanol.

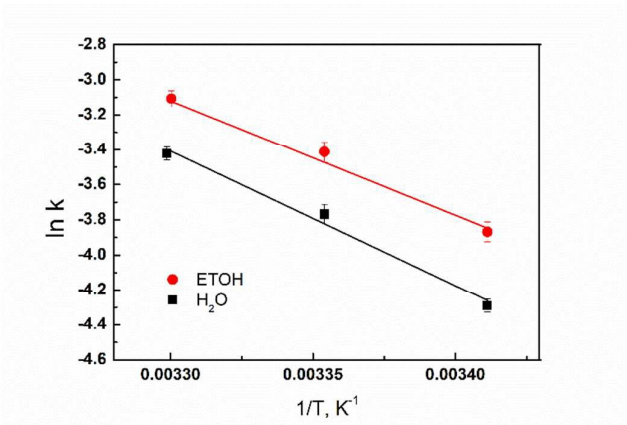

Figure 1. Arrhenius plot of the hydrogenation of bicarbonate and ethyl carbonate in presence of piperidine with 5 wt% Pd/AC in pure water and ethanol solvents, respectively. The reaction rates at different temperatures were shown in Supporting Information Fig S2. Reaction conditions: 1 M piperidine captured CO_2 in water or ethanol solutions, 400 psi H_2, 1.0 g of Pd/AC.

Besides studying the hydrogenation reactions, we also investigated the dehydrogenation of FPA to close the hydrogen storage / evolution cycle. We conducted the dehydrogenation of FPA (1 M in the aqueous solution with 70wt% ethanol) in the relatively high temperature range under the N_2 atmosphere with a pressure of 1 atm. As shown in Figure 2, as the reaction temperature increased to 80 °C, the yield of hydrogen reached ~82% after 40 minutes. At 100 °C, a 92.1% yield of hydrogen was achieved after 40 mins with a corresponding TOF of 9,908 h^{-1} within the initial 5 mins. The activation energy of the dehydrogenation was calculated to be 15 kJ/mol (Supporting Information Figure S3). By switching the aqueous ethanol solvent (70 wt% ethanol) to either pure water or absolute ethanol, however, the generation rate of H_2 gas from FPA became slower (Supporting Information Figure S4). Similar to that in the hydrogenation reaction, ethanol also exhibits the co-solvent promotion effect in the dehydrogenation reaction due to the improvement of solubility of reactants and intermediates, i.e., formats and ethyl carbonate. While by using the aqueous propanol solvent containing 70 wt% alcohol, the hydrogen yield achieved ~100% at 100 °C within only 30 mins (Supporting Information Figure S5) with a record fast rate (TOF = 1.21×10^4 h^{-1} within the initial 5 mins) for discharging this hydrogen battery system, which results in an equivalent power density of 77.8 W/kg. Besides hydrogen, nitrogen, and a minimal amount of CO_2, no other gas was detected (CO detection limit is < 1 ppm) (Supporting Information Figure S6). Thus, it was demonstrated that the same Pd/AC catalyst was active for reversible CO_2 hydrogenation / formate dehydrogenation by varying the pressure and the reaction temperature.

View Article Online
DOI: 10.1039/C8GC00954F

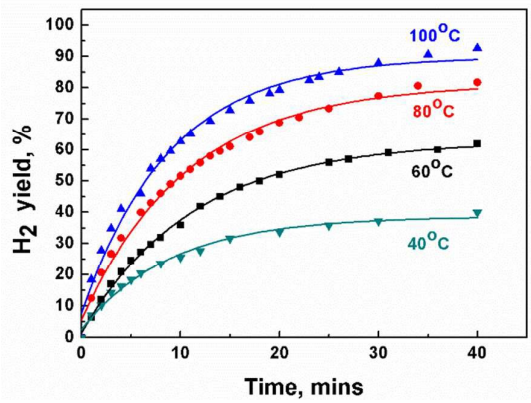

Figure 2. Effect of different temperatures on H_2 releasing rate from dehydrogenation of formate piperidine adducts. Reaction conditions: 0.1 g Pd/AC catalyst, 1 atm initial pressure of N_2, 1 M formate piperidine adducts, 20 mL aqueous solvent with 70% EtOH.

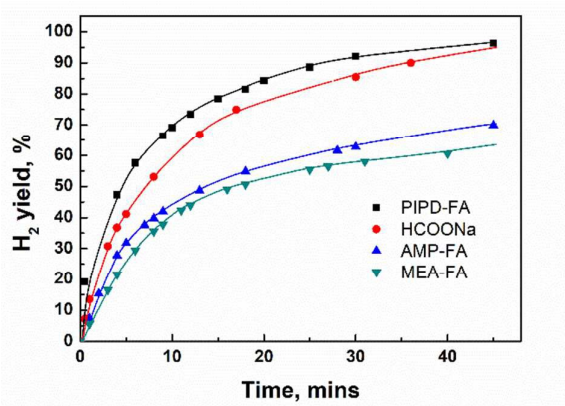

Figure 3. Effect of different bases on H_2 releasing rate from dehydrogenation of formate piperidine adducts. Reaction conditions: 1 M formic acid mixed with 1 M of varied bases, 20 mL aqueous solutions with 70% EtOH, 0.1 g Pd/AC catalyst, 1 atm initial pressure of N_2, 100 °C.

It is generally accepted that adding base additives promotes both CO_2 hydrogenation and formic acid dehydrogenation reactions.[2a, 7e, 22] Herein the effect of the loading amount of piperidine on the formate dehydrogenation rate was investigated by varying the concentration of piperidine from 0 M to 5 M. A drastic increase of the hydrogen yield was observed as the concentration of piperidine increased from 0 M to 1 M, but the yield of H_2 did not further increase with increasing the piperidine concentration from 1 M to 5 M (Supporting Information Figure S7). This observation indicates a typical marginal effect about piperidine: once the formate piperidine adducts were formed, the excessive piperidine did not enhance the dehydrogenation rate. We also investigated the effect of different base types with varied basicity strength on the formate dehydrogenation. As shown in Figure 3, the dehydrogenation rates with various bases were in the order of piperidine (pK_a=11.28) ≈ NaOH (pK_a=13.8) > AMP (pK_a=9.7) ≈ MEA (pK_a=9.5). It seems that given the same molar ratio of formic acid to the base, the higher pK_a of the base, the faster dehydrogenation rate was. From the thermodynamic point of view, the high pK_a of base would decrease the free energy for both hydrogenation and dehydrogenation reactions.[23]

The decomposition of formates may involve multiple steps. Here we used kinetic isotope effect (KIE) measurements with HCOOH and DCOOH to determine the rate-limiting step and to understand the indispensable role of piperidine in facilitating the dehydrogenation (Table 2). We hypothesize that transient formate species adsorb on the Pd surface followed by critical formate dissociation (Supporting Information Scheme S1). A general scheme of dehydrogenation of formic acid is through decarboxylation and thus CO_2 and H_2 are the final products. Adding an amine like piperidine would facilitate the conversion of formate amine adducts to bicarbonates or ethyl carbonates. The deuterium kinetic isotopic effect (KIE) was higher with DCOOH-piperidine-D_2O (KIE=2.1, Table 2, entry 4) than that with HCOOH-Piperidine-D_2O (KIE=1.1, Table 2, entry 2), showing that the cleavage of C-H bond in formate is the rate-limiting step for the decomposition of the FPA. Note that the conjugated acid of piperidine, in association with the piperidineH^+ ($PIPDH^+$) species formed via the reaction of piperidine with formic acid, as a proton donor can also facilitate the protonation of adsorbed formate species, leading to the formation of a Pd- bicarbonate / ethyl carbonate species during the dehydrogenation reaction. The Pd-bicarbonate/ ethylcarbonate complex might undergo further desorption from the Pd surface and become ionic species in the solvents.[24] At the elevated temperatures, bicarbonate or ethyl carbonate ions are readily decomposed to produce CO_2, which was detected in the dehydrogenation reactions at temperatures higher than 40 °C.

Table 2. Deuterium kinetic isotopic effect study. Reaction conditions: 10 mL 0.5 M PIPD-DCOOH or HCOOH solutions in H_2O or D_2O, 0.1 g Pd/AC catalyst, 0.1 MPa initial N_2 pressure, and 40 °C, 0-40 mins. Repeated three times.

Entry	Substrate/solvent	Reaction rate M s^{-1}	KIE
1	HCOOH-piperidine/H_2O	0.002076	1.0
2	HCOOH-piperidine/D_2O	0.001946	1.1
3	DCOOH-piperidine/H_2O	0.001297	1.6
4	DCOOH-piperidine/D_2O	0.000973	2.1

To get insight into the nature of surface intermediates during the FPA dehydrogenation reactions, the Pd/AC catalyst samples were further characterized during the reaction by *in-situ* ATR-FTIR. We first measured the IR spectra of the Pd/AC catalyst when flowing CO through the ATR cell to confirm the position of CO absorbance. A small peak was observed at ~ 2020 cm^{-1} (Supporting Information Figure S8), which can be assigned to linearly adsorbed CO.[25] We then measured the spectra of Pd/AC catalyst in the reactive environment for the dehydrogenation of FPA. Notably, as shown in Figure 4, no peak at 1800-2100 cm^{-1} (region of chemisorbed CO)[25] was observed during the dehydrogenation of FPA, which may be because piperidine suppressed the formation of CO. Boitiaux *et al.* also reported that piperidine had ligand effect and thus suppressed the CO formation during the hydrogenation reactions.[20] This is a crucial feature because CO could occupy the active sites on the Pd catalyst surface as a poisoner, and

View Article Online
DOI: 10.1039/C8GC00954F

consequently deactivate the catalyst. Also, no CO formation during H_2 evolution is indispensable in a PEM fuel cell since a trace amount of CO would poison the Pt cathode. In contrast, the CO peak was observed during the decomposition of monoethanolamine (MEA) - formate. The above observation suggests that piperidine could inhibit the undesired reaction to form CO, while largely promote the rate of H_2 generation. Note that the pKa of $PIPDH^+$ is 11.28, which is larger than that of $MEAH^+$ (pKa=9.45). Therefore the electron-donating ability of PIPD should be stronger than MEA. We speculate the stronger electron-donating ability could facilitate the CO desorption from the catalyst surface. Both the spectra with PIPD and MEA showed a negative peak at 1589 cm^{-1}, which is assigned to vibration of a surface-bound formate species,[26] indicating that the formate species on the catalyst surface were gradually consumed. Based on the intensity of this peak, the decomposition of formate with PIPD was completed in 40 mins since no further growth of this negative peak was detected after 40 mins. As for the spectra with MEA, the intensity of the peak at 1589 cm^{-1} reached to a plateau after 1 h. However, this peak is much smaller than that of piperidine which suggests that MEA formate adduct was not completely decomposed and instead, the reaction stopped (Supporting Information Figures S9 and S10). We thus conclude that, due to the CO poisoning, the Pd/AC catalyst for dehydrogenation of MEA-formate was deactivated with prolonged reaction time, which is consistent with the low yield of hydrogen as shown in Figure 3.

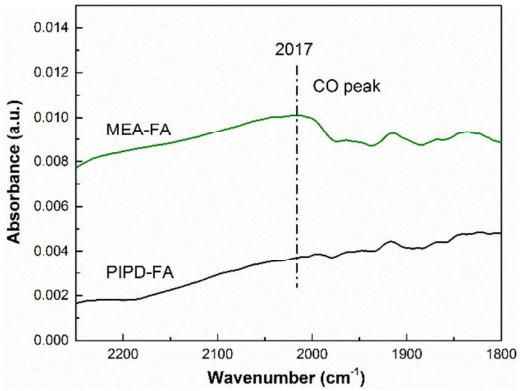

Figure 4. ATR-FTIR spectra measured during the dehydrogenation of formate with MEA and piperidine, respectively, at 55 °C.

As shown in Figures S8 and S9, the negative peaks at 1375 and 1346 cm^{-1} are ascribed to C-O vibration in HCO_3^-, $CH_3CH_2CO_3^-$ and $HCOO^-$, respectively, whose intensity increases with the reaction time. However, in the whole spectra, no C-N stretching vibration band (usually at ~ 1645 and 1518 cm^{-1})[27] was observed since there was no consumption or re-formation of piperidine, which indeed acted as a co-catalyst during the reaction. Note that these carbonyl compounds were likely displayed as monodentates[28] on the surface of the Pd catalyst in our reaction system (Scheme S1). In contrast, in a high-temperature gas-phase reaction, the bidentate forms of formate adsorbed on the Pd surface usually appear at higher wavenumbers.[25, 26a]

After 5 cycles of hydrogenation-dehydrogenation cycling tests, the loss of catalyst activities appeared to be negligible as shown in Figure 5. Moreover, piperidine did not decompose at 100 °C during the dehydrogenation reaction (Supporting Information Figure S11). The excellent stability of both the Pd/AC catalyst and the piperidine solvents suggests that the PFA based heterogeneously catalyzed hydrogen storage system is promising in terms of recyclability and reusability. Based on the current best H_2 production rates from this study (Table 1), to provide 1 kW of electric power would require 5.4 L of the 1 M piperidine formate solution or 0.69 L of the saturated piperidine formate solution (7.6 M at 25°C), using approximately 27 g of 5 wt% Pd/AC.

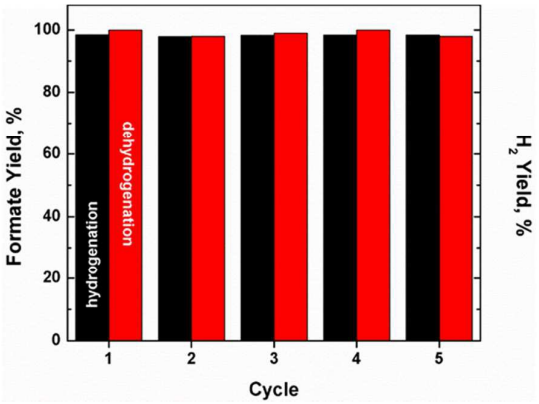

Figure 5. Stability test of Pd/AC catalyst for 5 cycles of hydrogenation-dehydrogenation. Hydrogenation of PIPD-CO_2: 70% 2-propanol, 0.1g Pd/AC, 30°C, 1 hour; Dehydrogenation of PIPD-Formic acid: 70% 2-propanol, 0.1g Pd/AC, 100 °C, 30 mins. The spent Pd/AC catalyst was reused without regeneration.

Conclusions

In conclusion, we demonstrated that a highly efficient reversible hydrogen storage approach can be realized based on the piperidine formate adducts, which is produced by hydrogenation of piperidine captured CO_2, in aqueous alcohol solutions. As for hydrogen charging, piperidine captured CO_2 shows the superior hydrogenation reactivity: ~ 95.5% formate yield could be obtained in the ethanol-water solution (70 wt% alcohol) with 400 psi H_2 after reacting for 1 hour at 30 °C. The kinetic rate of the reverse reaction, hydrogen discharging via dehydrogenation of the piperdine formate adduct in aqueous alcohol solutions, was also fast. The yield of high-purity H_2 reached ~100% in 40 mins at 100 °C. The impurities such as CO, NH_3 or piperidine were not detected in the discharged H_2. The deuterium kinetic isotopic study found that the cleavage of the C-H bond in the formate is the rate-limiting step. The mechanistic study by *in-situ* ATR-FTIR characterization discovered that piperidine improves both hydrogenation and dehydrogenation reactivity and no surface bound CO was formed during the dehydrogenation reactions. We also found that the Pd/AC catalyst is highly stable and easily to handle and recycle, so is piperidine. The storage of renewable energy can thus be realized through the "hydrogen battery", in which

View Article Online
DOI: 10.1039/C8GC00954F

the piperidine formate adduct solutions store the hydrogen generated via water splitting with electrical energy from renewable resources such as solar, wind, geothermal, etc.

Acknowledgements

This material is based upon work supported by the National Science Foundation under Grant No. CBET 1748579. The authors thank Dr. Steven Spain at the University of Nevada Reno for the chemical analysis using the NMR facilities in the Shared Instrumentation Laboratory (SIL). The authors also thank Drs. Zhenglong Li and Michael Hu at Oak Ridge National Laboratory for useful discussions.

Conflicts of interest

There are no conflicts to declare.

Notes and references

1 (a) IEA, *Technology Roadmap: Solar Photovoltaic Energy*, 2014; (b) GWEC, *Global wind statistics 2014*, 2015; (c) Q. Y. Bi, J. D. Lin, Y. M. Liu, X. L. Du, J. Q. Wang, H. Y. He and Y. Cao, *Angewandte Chemie - International Edition*, 2014, **53**, 13583–13587; (d) K. Christopher and R. Dimitrios, *Energy & Environmental Science*, 2012, **5**, 6640.

2 (a) S. Enthaler, J. von Langermann and T. Schmidt, *Energy & Environmental Science*, 2010, **3**, 1207; (b) J. Kothandaraman, M. Czaun, A. Goeppert, R. Haiges, J.-P. Jones, R. B. May, G. K. S. Prakash and G. a Olah, *ChemSusChem*, 2015, **8**, 1442–1451.

3 (a) G. Cau, D. Cocco, M. Petrollese, S. Knudsen Kær and C. Milan, *Energy Conversion and Management*, 2014, **87**, 820–831; (b) G. Gahleitner, *International Journal of Hydrogen Energy*, 2013, **38**, 2039–2061.

4 (a) L. Schlapbach and a Züttel, *Nature*, 2001, **414**, 353–358; (b) M. A. Rosen, *Hydrogen Production, Prospects and Processes.*, 2012, **1**, 10–29; (c) M. Yadav and Q. Xu, *Energy & Environmental Science*, 2012, 5, 9698–9725.

5 (a) J. Yang, A. Sudik, C. Wolverton and D. J. Siegel, *Chemical Society Reviews*, 2010, **39**, 656–675; (b) C. W. Hamilton, R. T. Baker, A. Staubitz and I. Manners, *Chemical Society Reviews*, 2009, **38**, 279–293; (c) K. M. Eblagon, D. Rentsch, O. Friedrichs, A. Remhof, A. Zuettel, A. J. Ramirez-Cuesta and S. C. Tsang, *International Journal of Hydrogen Energy*, 2010, **35**, 11609–11621; (d) W. Luo, P. G. Campbell, L. N. Zakharov and S.-Y. Liu, *Journal of the American Chemical Society*, 2011, **133**, 19326–19329.

6 (a) M. Grasemann and G. Laurenczy, *Energy & Environmental Science*, 2012, **5**, 8171; (b) P. Sponholz, D. Mellmann, H. Junge and M. Beller, *ChemSusChem*, 2013, **6**, 1172–1176; (c) F. Joó, *ChemSusChem*, 2008, **1**, 805–808.

7 (a) H. Horváth, G. Papp, R. Szabolcsi, Á. Kathõ and F. Joõ, *ChemSusChem*, 2015, **8**, 3036–3038; (b) Q. Liu, X. Yang, Y. Huang, S. Xu, X. Su, X. Pan, J. Xu, A. Wang, C. Liang, X. Wang and T. Zhang, *Energy Environ. Sci.*, 2015, **8**, 3204–3207; (c) K. Sordakis, A. F. Dalebrook and G. Laurenczy, *ChemCatChem*, 2015, **7**, 2332-2339; (d) J. Su, L. Yang, M. Lu and H. Lin, *ChemSusChem*, 2015, **8**, 813–816; (e) G. A. Filonenko, R. Van Putten, E. N. Schulpen, E. J. M. Hensen and E. A. Pidko, *ChemCatChem*, 2014, **6**, 1526–1530; (f) K. Jiang, K. Xu, S. Zou and W.-B. Cai, *Journal of the American Chemical Society*, 2014, **136**, 4861–4864; (g) S. F. Hsu, S. Rommel, P. Eversfield, K. Muller, E. Klemm, W. R. Thiel and B. Plietker, *Angewandte Chemie - International Edition*, 2014, **53**, 7074–7078; (h) P. Hu, E. Fogler, Y. Diskin-Posner, M. A. Iron and D. Milstein, *Nature Communications*, 2015, **6**, 6859; (i) P. Hu, Y. Ben-David and D. Milstein, *Angewandte Chemie - International Edition*, 2016, **55**, 1061–1064; (j) A. L. Wang, O. Naoya, K. Murata, T. Hirose, J. T. Muckerman, E. Fujita, Y. Himeda, L. Wang, N. Onishi, K. Murata, T. Hirose and J. T. Muckerman, *Chemsuschem,* 2017, **10**, 1071-1075; (k) D. Forberg, T. Schwob, M. Zaheer, M. Friedrich, N. Miyajima and R. Kempe, *Nature Communications*, 2016, **7**, 13201; (l) K. Koh, M. Jeon, D. M. Chevrier, P. Zhang, C. W. Yoon and T. Asefa, *Applied Catalysis B: Environmental*, 2017, **203**, 820-828; (m) D. Mellmann, P. Sponholz, H. Junge, M. Beller, J. Skea, N. Armaroli, V. Balzani, N. Armaroli, V. Balzani, N. Armaroli, et al., *Chem. Soc. Rev.* 2016, **45,** 3954–3988.

8 (a) A. Boddien, B. Loges, H. Junge, F. Gärtner, J. R. Noyes and M. Beller, *Advanced Synthesis and Catalysis*, 2009, **351**, 2517–2520; (b) B. Loges, A. Boddien, H. Junge and M. Beller, *Angewandte Chemie*, 2008, **47**, 3962–3965.

9 J. F. Hull, Y. Himeda, W.-H. Wang, B. Hashiguchi, R. Periana, D. J. Szalda, J. T. Muckerman and E. Fujita, *Nature chemistry*, 2012, **4**, 383–388.

10 G. Papp, J. Csorba, G. Laurenczy and F. Joó, *Angewandte Chemie*, 2011, **50**, 10433–10435.

11 Q.-Y. Bi, J.-D. Lin, Y.-M. Liu, X.-L. Du, J.-Q. Wang, H.-Y. He and Y. Cao, *Angewandte Chemie*, 2014, **53**, 13583–13587.

12 E. Hosono, T. Kudo, I. Honma, H. Matsuda and H. Zhou, *Nano Letters*, 2009, **9**, 1045–1051.

13 J. Su, M. Lu and H. Lin, *Green Chemistry*, 2015, **17**, 2769–2773.

14 W. H. Wang, S. Xu, Y. Manaka, Y. Suna, H. Kambayashi, J. T. Muckerman, E. Fujita and Y. Himeda, *ChemSusChem*, 2014, **7**, 1976–1983.

15 R. M. Deshpande, R. V. Chaudhari and H. Delmas, *Journal of Chemical & Engineering Data*, 1996, **41**, 1414–1417.

16 P. Holms, M. NAAZ, B. Poling, *Industrial & Engineering Chemistry Research*, 1998, **37**, 3281-3287.

17 (a) G. A. Filonenko, M. P. Conley, C. Copéret, M. Lutz, E. J. M. Hensen and E. A. Pidko, *ACS Catalysis*, 2013, **3**, 2522–2526; (b) P. G. Jessop, Y. Hsiao, T. Ikariya and R. Noyori, *J. Am. Chem. Soc.,* 1996, **118**, 344–355; (c) Z. Xu, N. D. Mcnamara, G. T. Neumann, W. F. Schneider and J. C. Hicks, *ChemCatChem*, 2013, **5**, 1769–1771.

18 P. V. Kortunov, L. S. Baugh, M. Siskin and D. C. Calabro, *Energy & Fuels*, 2015, **29**, 5967–5989.

19 (a) K. Robinson, A. McCluskey and M. I. Attalla, *Chemphyschem*, 2011, **12**, 1088–1099; (b) P. V. Kortunov, M. Siskin, L. S. Baugh and D. C. Calabro, *Energy & Fuels*,

View Article Online
DOI: 10.1039/C8GC00954F

2015, **29**, 5919–5939.

20 J. Boitiaux, J. Cosyns and S. Vasudevan, *Applied Catalysis*, 1985, **15**, 317–326.

21 (a) H. Wiener, Y. Sasson and J. Blum, *Journal of Molecualr catalysis*, 1986, **35**, 277–284; (b) B. Zaidman, H. Wiener and Y. Sasson, *International Journal of Hydrogen Energy*, 1986, **11**, 341–347; (c) B. Zaidman; H. wiener; Y. Sasson, *solar energy*, 1989, 291–296.

22 Z. Zhang, S. Hu, J. Song, W. Li, G. Yang and B. Han, *ChemSusChem*, 2009, **2**, 234–238.

23 D. B. Lao, B. R. Galan, J. C. Linehan and D. J. Heldebrant, *Green Chem*, 2016, **18**, 4871-4874.

24 Q. Bi, X. Du, L. He, Y. Liu, Y. Cao, H. He and K. Fan, *Journal of the American Chemical Society*, 2012, **134**, 8926–8933.

25 G. C. Cabilla, A. L. Bonivardi and M. A. Baltanàs, *Journal of Catalysis*, 2001, **201**, 213–220.

26 (a) V. Arunajatesan, B. Subramaniam, K. W. Hutchenson and F. E. Herkes, *Chemical Engineering Science*, 2007, **62**, 5062–5069; (b) J. Araña, C. Garriga I Cabo, J. M. Doña-Rodríguez, O. González-Díaz, J. A. Herrera-Melián and J. Pérez-Peña, *Applied Surface Science*, 2004, **239**, 60–71.

27 (a) K. Robinson, A. McCluskey and M. I. Attalla, *Chemphyschem : a European journal of chemical physics and physical chemistry*, 2011, **12**, 1088–1099; (b) G. Richner and G. Puxty, *Ind Eng Chem Res*, 2012, **51**, 14317–14324.

28 A. C. C. Chang, S. S. C. Chuang, M. Gray and Y. Soong, *Energy and Fuels*, 2003, **17**, 468–473.